Journal of Mines, Metals and Fuels, *73(3): 695-708; 2025. DOI: 10.18311/jmmf/2025/47817*

Print ISSN : 0022-2755

Journal of Mines, Metals and Fuels

Contents available at: *www.informaticsjournals.co.in/index.php/jmmf*

Improvement of Torsional Rigidity of Steel Supporting Structure Topside Module

Adinath Yadhav*, Mrudula Kulkarni and Devendrakumar Ingale

Dr. Vishwanath Karad MIT World Peace University, Pune - 411038, Maharashtra, India; adinath.yadhav@mitwpu.edu.in

Abstract

The study investigates the improvement of torsional rigidity in floating support structures, focusing on the offshore industry's structural integrity needs. Offshore platforms, such as Floating Production Storage and Offloading (FPSO) units, face challenges due to dynamic environmental loads and long-term corrosion effects, which compromise structural rigidity and stability. To address these issues, the research evaluates multiple factors affecting torsional rigidity, including bracing configurations, material selection, and cross-sectional dimensions of structural components. The study utilizes STAAD Pro software to analyze FPSO structures under various loading conditions, including wind, wave, and operational loads, to identify critical torsional responses. Various bracing configurations were tested, with a focus on knee bracing patterns, which showed significant potential in enhancing structural stiffness and minimizing torsional deformation. Empirical data demonstrated that knee bracing effectively improves torsional performance by reducing displacement and increasing modal frequencies across a range of section sizes. By optimizing the unbraced length ratio (a/L), the study highlights that larger sections with strategic bracing offer improved rigidity and vibration resistance, crucial for offshore stability under dynamic loading conditions. Recommendations from this research support industry-standard load combinations, providing a practical approach to enhancing torsional rigidity in floating offshore platforms. The findings contribute valuable insights into design optimization, promoting safer and more resilient offshore infrastructure.

Major Findings: *Knee bracing significantly improves torsional rigidity by reducing displacement and increasing modal frequencies. Improving torsional rigidity contribute to greater structural stiffness and vibration resistance, making structure more stable and resilient to dynamic environmental forces, particularly in harsh offshore conditions.*

Keywords: *Analysis and Design, Bracings, Offshore Structures, Steel Structure, Torsional Rigidity*

1.0 Introduction

Offshore platforms are typically constructed using advanced materials such as specialized alloys and high-grade corrosion-resistant steel, chosen for their strength and durability. Despite this, inadequate structural rigidity played a critical role in this collapse. Offshore structures are continuously exposed to dynamic loads, including inertia forces as well as wave and wind forces, which can trigger various failure mechanisms like fatigue, joint loosening, and corrosion[1]. These factors collectively diminish the structures stiffness over time, potentially leading to catastrophic component failure and posing serious risks to the projects success. Although offshore structures are typically designed with a lifespan of 40 to 50 years, many of their components are highly susceptible to corrosion (Figure 1). This gradual deterioration reduces rigidity and undermines stability, ultimately resulting in structural failure over time[2].

**Author for correspondence*



Figure 1. Failure of offshore platform.

Engineering design experts from various offshore industries provided insights on the importance of emphasizing torsional rigidity in offshore structures, based on challenges they have encountered in the field[3]. Key points identified during the research engagement include the need to address structural integrity, fatigue resistance, vibration control, operational stability, wind and wave loading, dynamic responses to extreme events, interactions with piping and equipment, and ensuring regulatory compliance[4].

A novel theory has been devised to estimate the elastic lateral-torsional buckling strength of steel beams or columns reinforced with one or more GRP laminates bonded with an adhesive layer. The proposed theory accounts for GRP laminates orthotropic properties by taking into consideration different fiber orientations, ply quality, and the partial interaction between steel and GRP laminates[5]. Parametric studies show that the stacking sequences of Glass Fiber Reinforced Polymer (GFRP) laminates, GFRP shear and elastic moduli, and adhesive shear moduli all have a substantial influence on the structures elastic buckling resistance[6]. The study used experimental analysis to explore the torsional behaviour of GFRP- Reinforced Concrete (RC) pontoon decks, with an emphasis on rotational direction, reinforcing bar distribution, and edge cuts[7]. The findings revealed that the arrangement of reinforcing bars affected both the torsional capacity and failure patterns of GFRP-reinforced concrete decks under torsional loading. In the post-cracking stage, decks with double-layer reinforcement displayed slower and narrower crack propagation than those with single-layer reinforcement[8]. The author examined a retrofit design that involved the installation of Buckling-Restrained Braces (BRBs), which successfully decoupled the buildings torsionally coupled lateral modes[9]. This led to a reduction in torsional response, residual displacement and inter- storey drift in the "soft storey". The study concluded that this retrofit design significantly enhanced the overall structural performance, reduced lateral response, and increased the buildings safety and resilience to seismic events[10]. The study focuses on the torsional analysis of steel components with thin-walled open cross-sections, with the special goal of identifying the corresponding stresses. Three approaches are presented: Vlasov theory, modified bending and torsion analogies, and simplified methods based on pair forces. To examine the influence of torsion on a steel crane girder, the study compares various analytical methodologies[11].

The study investigated the torsional behaviour of Square Tubed Reinforced Concrete (STRC) specimens, which were simulated and validated with ABAQUS finite element software[12]. The modelling results were then compared with experimental data on ultimate torsional capacity and failure modes[13]. This work gives a complete parametric analysis of essential structural elements, such as steel tube yield strength, thickness, cross-section dimensions, concrete strength, longitudinal reinforcement, and stirrups, to determine their impact on STRC column torsional capacity[14].

The seismic behavior of reinforced concrete structures was studied utilizing lead-core rubber elastomeric bearing base isolators and a curved surface friction pendulum slider[15]. The research, which was carried out on 3D models of varied heights, took into account the structural parts nonlinear behaviour. The data show that when the base isolator systems centre of stiffness is not aligned with the mass centre, torsional eccentricity produces the maximum torsional irregularity coefficient[16]. This study looks into the impact of steel brace buckling on the in elastic torsion of a concrete frame structure reinforced with steel bracing. Two structural models underwent laboratory shake table tests: One with standard bracing and the other with buckling-restrained bracing. Additionally, finite element analysis models

were created to mimic the effects of buckling[17]. The data show that the dynamic buckling hypothesis, which involves both inertial force and inertial torsional moment acting on the structure, is more feasible than competing theories[18].

A 10,000 TEU (Twenty-Foot Equivalent Unit) container ship, which has a huge deck aperture and less torsional rigidity than conventional ships, is the subject of this study's investigation into its torsional behaviour and maximum strength[19]. The collapse behaviour of the structure was examined using both model experiments and numerical simulations, with a particular emphasis on warping and shear buckling deformations. The results show that the side shells yielding and shear buckling are the main reasons why the hull girder fails under pure torsion[20]. To replicate the torsional restriction at the cross-bracing angle section link, an end restraint device was created and fitted with springs[21]. 105 pieces with equal leg angles served as bracing elements in the experiment. This study assessed the specimens failure modes and stability, finding a positive correlation between the stability of the equal angle sections and the stiffness of the end constraint. The study also looked at how column bending stiffness and stability were affected by the ratio of torsional stiffness at nodes and the slenderness ratio; the results were validated experimentally and by FEM simulations[22].

With this background and numerous discussions with offshore industries (Design Engineers) following points are highlighted. This research focuses on following points.

- Rigidity analysis of floating offshore structures topside module.
- Parameters responsible for calculating rigidity of floating offshore platforms.
- Approach to improve the rigidity of floating offshore platforms.

2.0 Methodology

The current research focuses on a Floating Production Storage and Offloading (FPSO) platform, which is designed to receive production from subsea oil wells. This FPSO will include processing facilities to treat fluids from subsea production, stabilize them, and separate produced water and natural gas. The FPSO consists

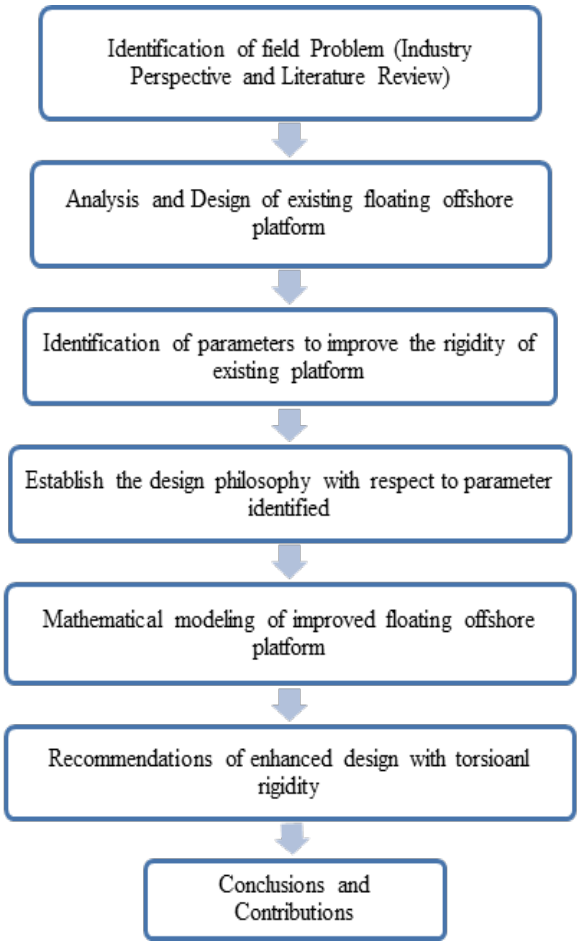


Figure 2. Methodology.

of several modules, each with distinct applications, equipment, pipelines, and electrical load distributions. For this study, the module highlighted in red in the Figure 3 is selected. The dimensions of Module 1C are 20.89 meters in length, 14.60 meters in breadth, and 18 meters in height from the stool level. The Figure 2 illustrates the flowchart of methodology adopted in the research work.

The design utilizes structural steel types 1H, 2H, 3H, and 3M, all compliant with the material specifications established by the American Institute of Steel Construction (AISC). Each steel type is chosen for its specific mechanical properties and performance characteristics, including yield strength, ductility, and fatigue resistance, making them appropriate for various components of the structure. By adhering to AISC standards, the materials employed in the design meet

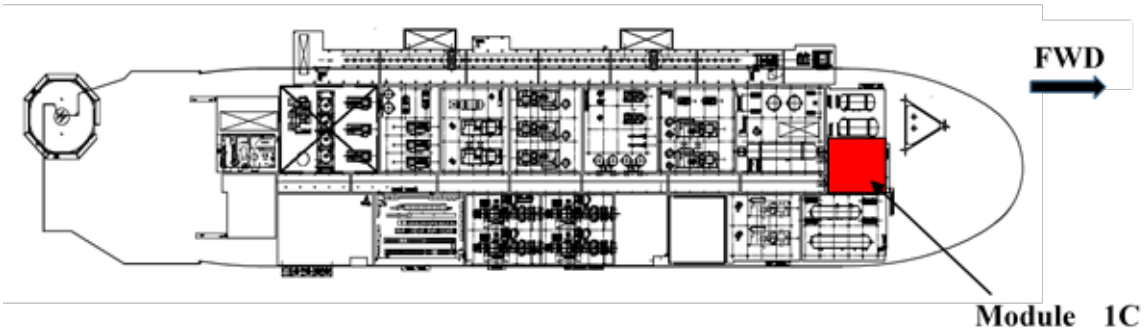


Figure 3. FPSO detailed plan view.

rigorous industry requirements for safety, reliability, and structural performance.

2.1 Design Loads

STAAD programs used to conduct the analyses. This section lists and summarizes the structural analysis done. The current structural design can survive all conditions associated with in-place, lifting, and weighing structural studies, as specified by API-RP 2A-WSD and AISC - ASD. This section describes the basic load cases used in these analyses, which include the structures Modelled Self-Weight (MSW), Non-Modeled Weights (NMSW), and discipline-specific loads such as mechanical (dry and operating), piping (dry and operating), electrical, and instrumentation. Additionally, the analyses take into account motion- induced accelerations, hull deformations (hog and sag), and wind loads. Table 1 shows the weight load and its contingencies based on API requirements.

STAAD Pro uses basic weight groups to properly control and organize the varied variety of loads acting on an offshore structure. By categorizing these loads, engineers may more efficiently apply and combine them during structural analysis, guaranteeing that the design stays safe and efficient across a variety of operational and exceptional situations. This technique allows for systematic load application, simplifies load combination, and provides adequate structural optimization for complex offshore structures. Figure 4 depicts the placement of various equipment (designated by alphanumeric codes) and their load distribution within the platforms structural framework in an isometric perspective. The green arrows above the various components represent the applied loads or forces operating on the structure, indicating the places at which equipment loads will be transferred to the overall structure. The red elements are dummy components employed in STAAD Pro to ensure

Table 1. Weight load and contingencies

Load Case	Dry Weight Without -Contingency, (kN)	As per API Contingency (%)	Total, (kN)
Modelled-Structural Weight (MSW)	1495	4	1555
Non-Modelled -Structural Weight (NMSW)	310	0	310
Mechanical-Operating Weight (MOW)	1653	10	1818
Piping-Operating Weight (POW)	724	0	724
Electrical and Instrumental Weight (EIW)	165	0	165
Total	2788		3019

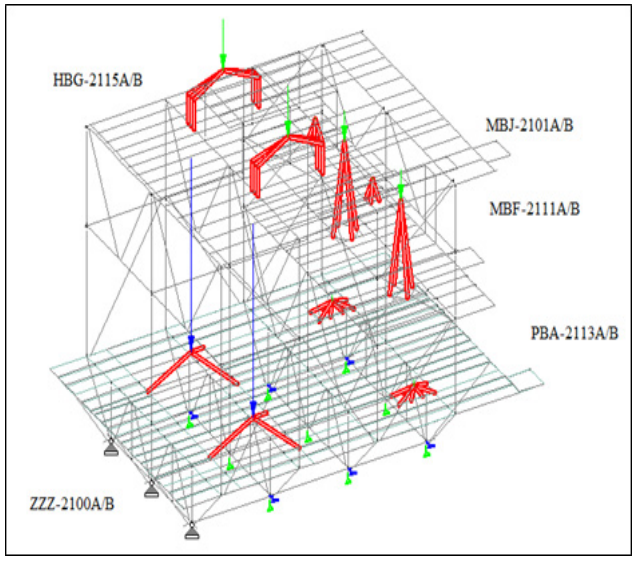


Figure 4. Equipment positioning details.

Table 2. Acceleration factors

Dire.	Acceleration	Normal Condition	Extreme Condition
Head	(±) a_x	0.088	0.0981
	(±) a_y	0.27	0.331
	(±) a_z	-	-
Beam	(±) a_x	-	-
	(±) a_y	0.27	0.331
	(±) a_z	0.26	0.531
Quarter	(±) a_x	0.06	0.07
	(±) a_y	0.27	0.331
	(±) a_z	0.18	0.37

a more consistent load distribution across structural members.

The STAAD program is used to model the inertial loads produced by unit accelerations (1.0g) in the global X, Y, and Z directions. These unit accelerations are then paired with motion-induced load factors calculated from site-specific variables to precisely depict the environmental pressures that the structure will face. The details of acceleration factors are shown in Table 2.

API standards, such as API RP 2A and API RP 2T, provide guidance for assessing and applying environmental loads, including wind speeds, to offshore constructions. Table 3 shows the design wind speeds for several design situations at 10 meters above mean sea level.

The normal and extreme operating accelerations in the Y, X and Z directions for various weight groups, as outlined in the table, represent the lateral accelerations experienced by different components of the offshore structure during routine operations and critical conditions. This acceleration data is essential for ensuring that the structure can withstand dynamic forces without excessive movement or vibrations, which could compromise safety, operational efficiency, and the integrity of sensitive equipment. The different weight groups created for analysis are summarized in Table 4.

2.2 Load Combinations

Commonly accepted load combinations for normal operating conditions adhere to guidelines established by international codes, such as those from the American Institute of Steel Construction (AISC) and API standards. Typical combinations include:

Table 3. Wind speed for various conditions

Design Condition	Return Period(years)	Design Wind at (10m above MSL)		Basic Wind Speed (10m above MSL)
		Speed	Avg. Time	
Normal Operating Condition (NOC)	10 years	27.52 m/s	10 mins	25.23 m/s
Extreme Operating Condition (EOC)	100 years	34.61 m/s	10 mins	31.45 m/s

Table 4. Weight groups for load combinations

STAADs - Load Case Name	Description	Weight Groups Considered
NOAX/ EOAX	Acceleration in X direction for normal or extreme operating condition.	MSW
		NMSW
		MOW
		POW
		EIW
NOAY/ EOAY	Acceleration in Y direction for normal or extreme operating condition.	MSW
		NMSW
		MOW
		POW
		EIW
NOAZ/ EOAZ	Acceleration in Z direction for normal or extreme operating condition.	MSW
		NMSW
		MOW
		POW
		EIW

DL + WL (Dead load plus wind load)

DL + LL + WL (Combination of dead load, live load, and wind load)

DL + LL + WL + $DL_{dynamic}$ (Inclusion of dynamic loads along with dead, live, and wind loads)

Given the variety of loads present on the FPSO platform, accurate findings necessitate analyzing load combinations in reference to the load cases and groups discussed previously. Structural analysis of FPSO's considers all potential load permutations and combinations to identify critical load scenarios that may impact structural integrity. By systematically merging existing load cases, weight groups, and other loads across different scenarios (both normal and extreme), it becomes easier to identify the most significant load cases that induce maximum stress or deformation in the structure. A total of 160 load combinations were studied for the considered structure based on various weight groups and load cases, with a sample load combination presented in the table below. A sample load combinations are shown in Table 5. Combination load case name and load case no. are taken as per STAAD analysis report.

Table 5. Sample load combinations

Combination L/C Name	Load Case No.	Primary L/C Name	Factor
1001	2	WLOC	1.00
	3	NOAX	0.09
	5	NOAY	0.28
	15	NWPX	1.00
	31	SAGS (IN PLACE)	1.00
1002	2	WLOC	1.00
	3	NOAX	0.09
	5	NOAY	0.28
	16	NWPZ	1.00
	31	SAGS (IN PLACE)	1.00

2.3 Section Summary

All the sections used for design of structure mentioned are taken as per AISC standards are tabulated in Table 6.

The Figure 5 shows the detailed view of FPSO with member properties as mentioned in Table 5. The analysis model includes all primary and secondary members

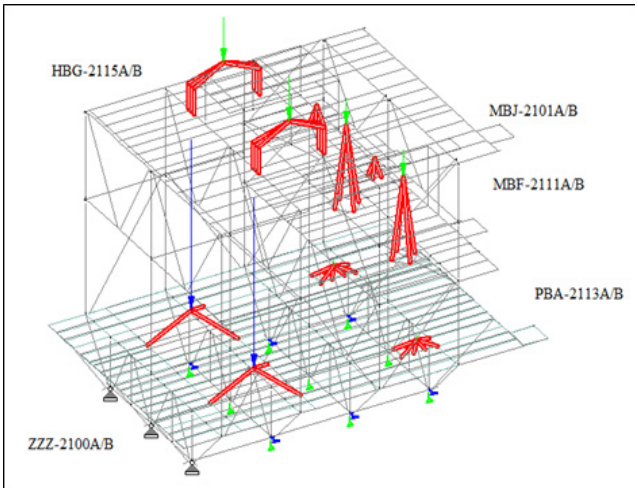


Figure 5. Isometric view of FPSO supporting structure.

Table 6. Section summary

Ref. No in STAAD	Section	OD (mm)	Web/Plate Thickness (mm)	E N/mm²	G N/mm²	Fy N/mm²	Density kg/m³
R1	Plate		8	205 x 10^3	80 x 10^3	325 x 10^3	7833.41
R2	Pipe (Dummy)	200	-	205 x 10^3	80 x 10^3	0	0.010
R3	Pipe	273	-	205 x 10^3	80 x 10^3	325 x 10^3	7833.41
R4	Pipe	219	-	205 x 10^3	80 x 10^3	325 x 10^3	7833.41
R5	HW 200x200		8	205 x 10^3	80 x 10^3	325 x 10^3	7833.41
R6	HW 300x300		10	205 x 10^3	80 x 10^3	325 x 10^3	7833.41
R7	HW 150x150		7	205 x 10^3	80 x 10^3	325 x 10^3	7833.41
R8	HM 340x 350		9	205 x 10^3	80 x 10^3	325 x 10^3	7833.41
R9	HM 390x300		10	205 x 10^3	80 x 10^3	325 x 10^3	7833.41
R15	HM 244x175		7	205 x 10^3	80 x 10^3	325 x 10^3	7833.41
R16	HM 294x200		8	205 x 10^3	80 x 10^3	325 x 10^3	7833.41
R17	HN 300x150		7	205 x 10^3	80 x 10^3	325 x 10^3	7833.41
R18	Taper HM 340x250		20	205 x 10^3	80 x 10^3	325 x 10^3	7833.41
R19	HW 250x250		8	205 x 10^3	80 x 10^3	325 x 10^3	7833.41

that contribute to the overall stability and stiffness of the structural system, with offsets and eccentricities appropriately applied. Deck plates are also integrated to account for in-plane rigidity.

2.4 Parameters Governing Torsional Rigidity

After reviewing existing research papers, case studies, and consulting with industry experts, several parameters contributing to torsional rigidity were identified and examined for feasibility. The key parameters include:

1. Bracing relative to the load path throughout the structure.
2. Strength-to-weight ratio of structural elements.
3. Optimal span and height of structural elements based on their functions.
4. Use of composite materials for enhanced durability.
5. Moment-resistant portal frames.
6. Tapered profiles for sections where feasible.

Among these identified parameters, various bracing patterns have emerged as the most effective means for enhancing the torsional rigidity of the structure,

according to industry experts. This preference is rooted in the practicality and feasibility of implementing different bracing configurations in the field. Bracing systems are crucial for improving the overall stiffness of the structure by providing additional resistance to twisting and rotational forces. Well-designed bracing adheres to the load path, offering lateral and torsional support by tying the structure together and preventing excessive twisting.

2.5 Implementation of Knee Bracing

From the parameters identified, the knee bracing pattern has been selected as the most feasible option from an industry perspective, particularly concerning the load path within the structure. In this chapter, various bracing patterns are examined for primary flexural and compression elements of the chosen case study model. To determine the optimal location for bracing, twisting, mode shapes, and natural frequencies are analyzed in detail. Additionally, various section sizes are evaluated through different trials to identify the most optimized and preferred section size for the bracing system. For each bracing location, the distance from one support is measured and designated as "a". To graphically represent the results, the a/L ratio is calculated for each scenario.

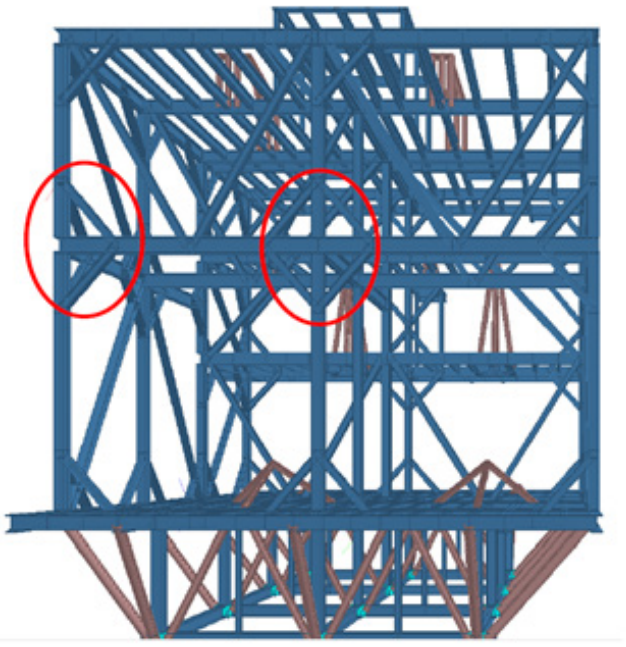


Figure 6. FPSO bracing location details.

Figure 6 illustrates a structural frame, with the knee bracing system highlighted in red circles at critical points. Knee bracing consists of diagonal members connected near the joint between the beam and column, enhancing the frame's stiffness and stability. These braces are strategically positioned to minimize torsional deformation, distributing forces more evenly throughout the structure, thereby reducing stress concentrations in individual members and improving overall torsional resistance. Various trials are conducted to determine the optimal location for the bracing pattern to effectively counteract torsion in the structure. To establish the ideal bracing pattern, the placement of knee braces is varied along the longitudinal direction of the structural members, and the structure is analyzed concerning its torsion mode.

3.0 Results and Discussions

3.1 Torsional Rigidity with HW 150X 150

Figure 7 presents a comprehensive empirical analysis of the impact of knee bracing on the torsional rigidity of structures. The results indicate that knee bracing becomes increasingly effective in stabilizing the structure as the modal frequency rises, suggesting enhanced stiffness and reduced flexibility under dynamic loading conditions. As the frequency increases (up to approximately 6.5 Hz), the structure experiences improved bracing effectiveness, achieving near-full engagement of the brace ($a/L \approx 0.35$).

Furthermore, as the modal frequency increases from about 4.5 Hz to 6.5 Hz, the torsion mode number escalates from 3 to 7, indicating that the system becomes more resistant to twisting and torsional effects.

3.2 Torsional Rigidity with HW 200X 200

Higher modal frequencies are associated with stiffer modes of vibration, where the structure resists deformation more efficiently. Figure 8 suggests that knee bracing is progressively resisting higher frequencies, but with greater deformation as frequency increases.

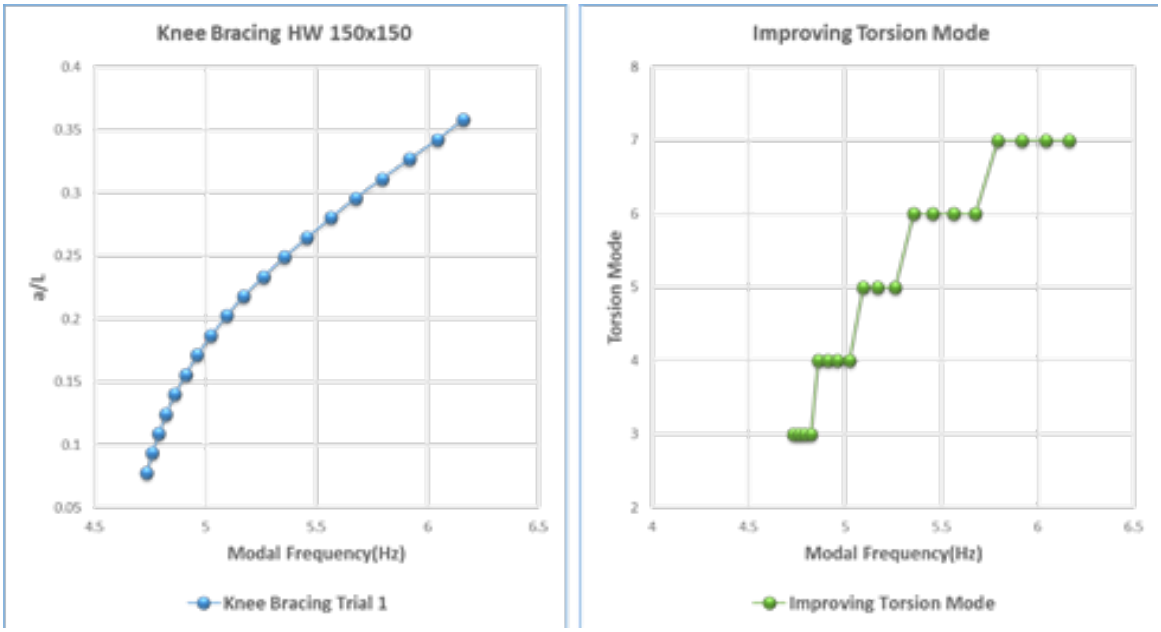


Figure 7. Torsional rigidity with HW 150 x 150.

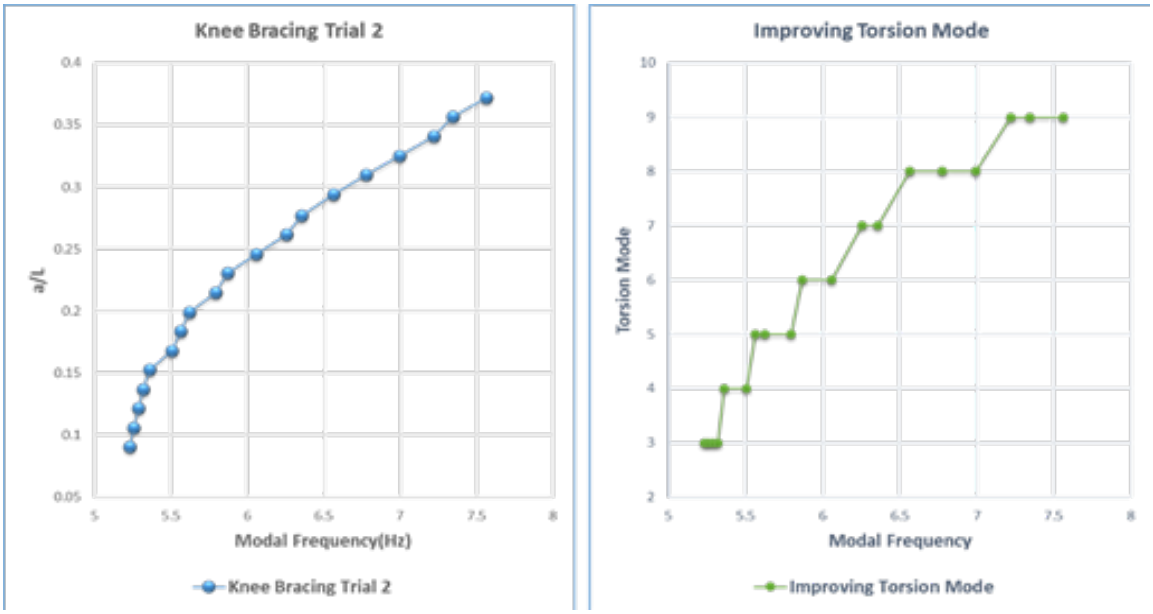


Figure 8. Torsional rigidity with HW 200 x 200.

3.3 Torsional Rigidity with HW 225 X 225

Figure 9 illustrates an increasing relationship between modal frequency and the ratio a/L. At lower frequencies (6 Hz to 7 Hz), there is a steeper rise in displacement compared to higher frequencies. After 7 Hz, the rate of increase in a/L becomes more linear and moderate up to about 10 Hz. The curves general upward trend indicates that as the structure vibrates at higher frequencies, its normalized deformation increases, which is typical in dynamic analyses. For torsion mode at lower frequencies (6 Hz to 7 Hz), the structure transitions through lower torsional modes (around mode 3 to mode 5). At frequencies around 7.5 Hz to 10 Hz, the structure transitions through higher torsional modes (up to mode 10).

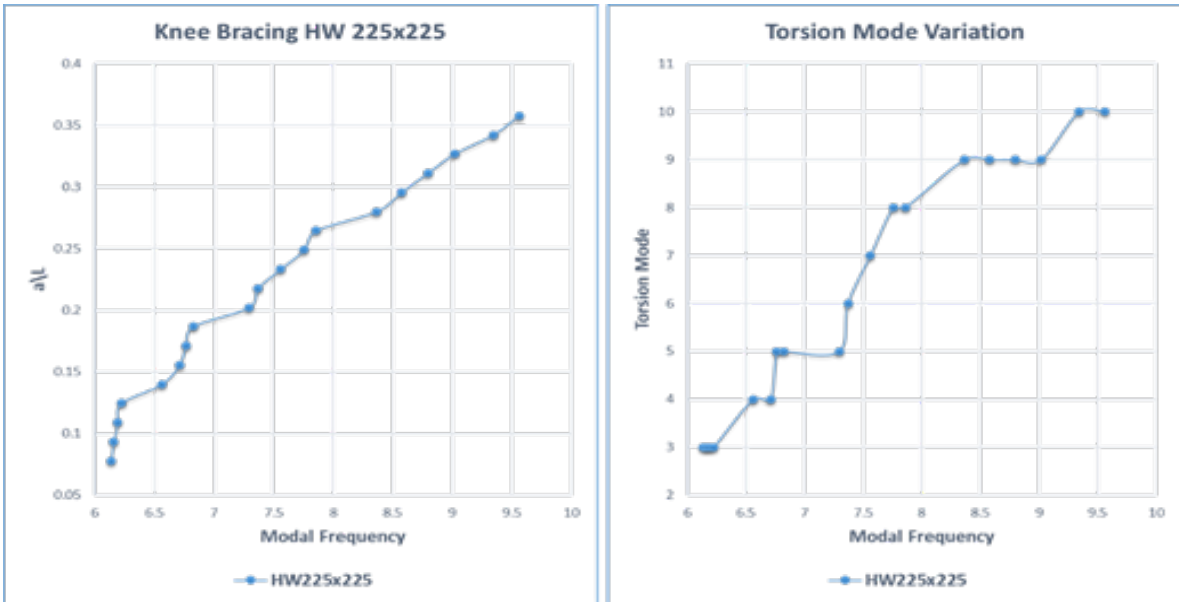


Figure 9. Torsional rigidity with HW 225 x 225.

3.4 Torsional Rigidity with HW 250 X 250

Figure 10 shows that the curve becomes steeper from frequency 9 to 10, where ΔL increases significantly to around 0.25. After this, there is a slower but steady rise, reaching a peak ΔL value of approximately 0.37 at a modal frequency of 12.8. At a frequency of 7, the torsion mode starts at about 4. A significant jump occurs around frequency 8, where the torsion mode increases to 6. Finally, at a modal frequency of around 12.8, the torsion mode increases further, reaching a maximum of 12.

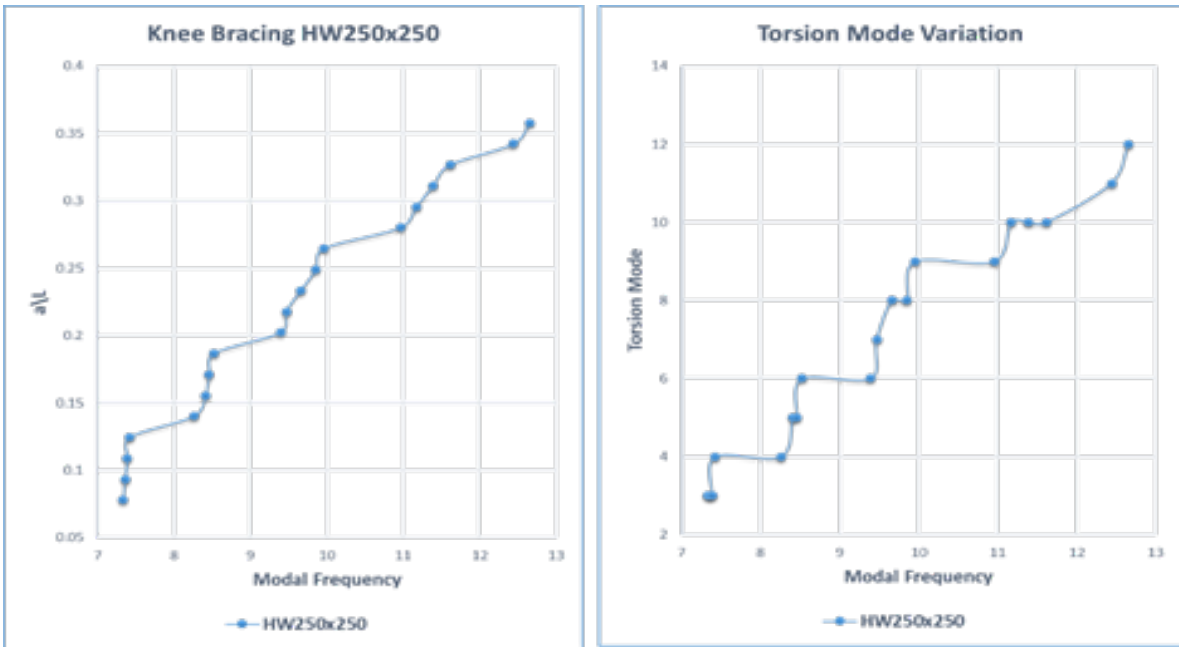


Figure 10. Torsional rigidity with HW 250 x 250.

3.5 Torsional Rigidity with HW 300 X 300

The Figure 11 suggests that improving the a/*L* ratio through different trial values has a significant impact on the systems torsional rigidity. So, for the section HW 250 x 250 and HW 300 x 300 the maximum torsion mode could delayed is up to 12. Overall, this indicates that optimizing the a/*L* ratio can enhance the torsional rigidity of the structure, especially at higher modal frequencies, providing improved performance and stability.

3.6 Mode Frequency with Bracing Pattern

Figure 12 is the compilation of results of all individual

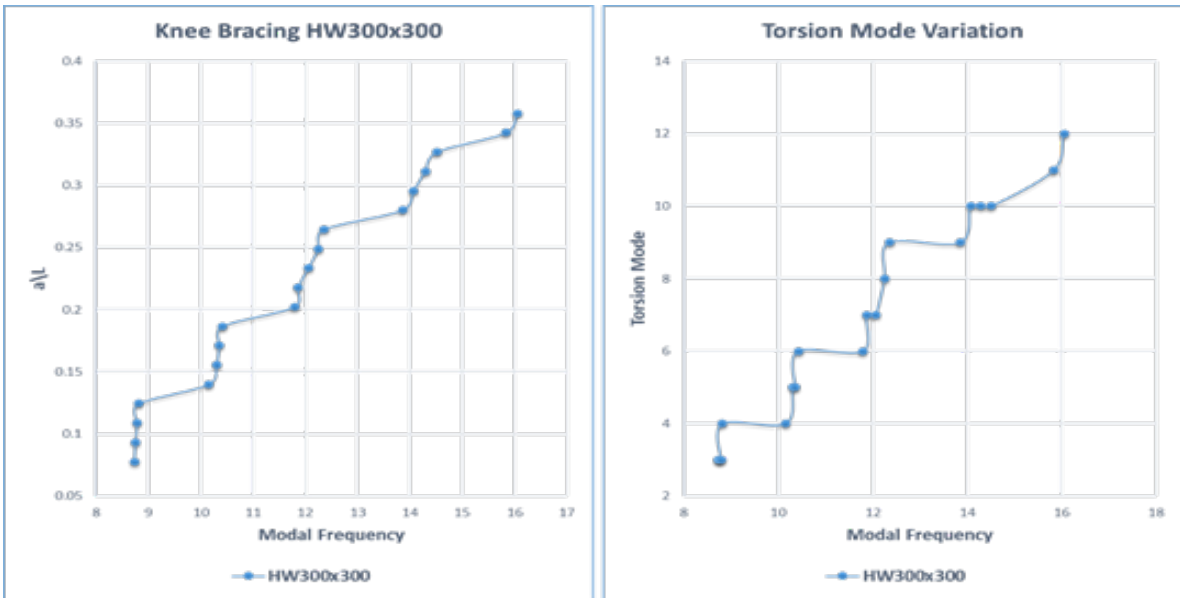


Figure 11. Torsional rigidity with HW 300 x 300.

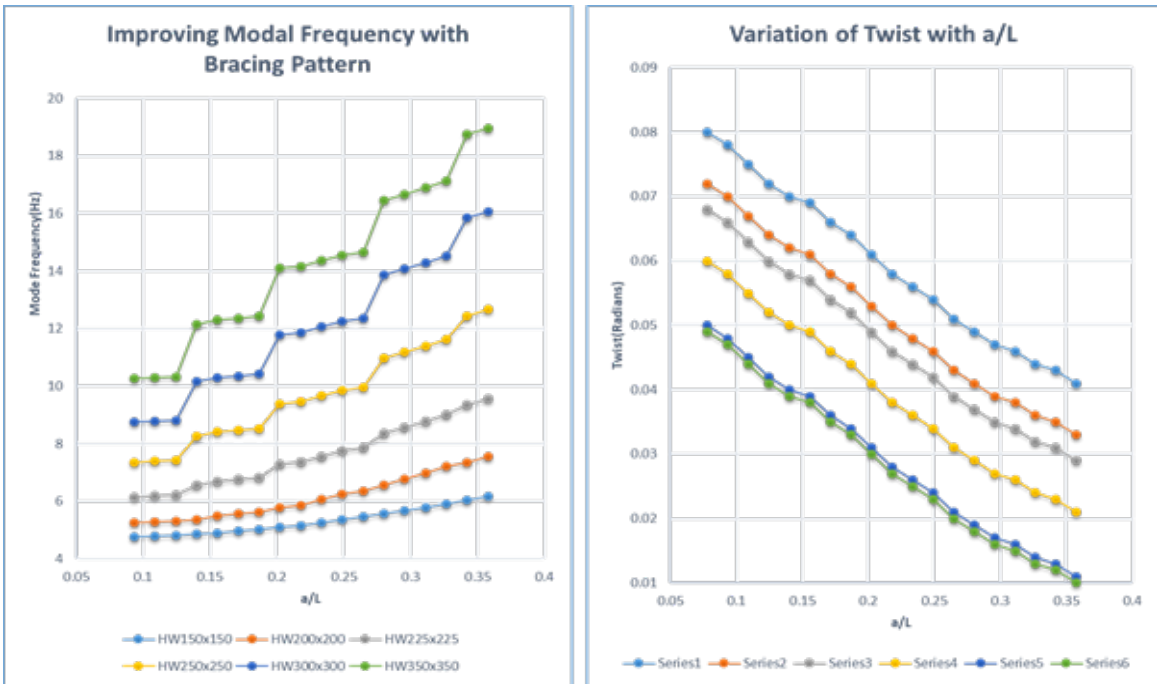


Figure 12. Mode frequency with bracing pattern.

attempted section for the bracing. It shows the betterment of section for the bracing based on the torsion mode, twist and modal frequency. Section HW 350 x HW 350 is always better for the bracing with maximum torsion mode 12 and almost negligible twisting in the overall structure. Figure 11 shows the effects of knee bracing on the torsional rigidity of structural elements. Through detailed empirical data, including torsional stiffness coefficients and angular displacements, the study showcases how the application of knee bracing in structures, such as HW 150 x 150, HW 200 x 200, HW 250 x 250, HW 300 x 300 and HW 350 x HW 350 and others enhances torsional performance. The provided values highlight the progressive increase in torsional rigidity with the introduction of knee bracing, indicating its effectiveness in resisting torsional loads.

4.0 Conclusions

Influence of Bracing Patterns: As the unbraced length (a/L) increases, the modal frequency rises for all sections. This suggests that extending the unbraced length leads to higher natural frequencies due to the bracing configuration. However, this effect is more pronounced in larger sections, where the increase in modal frequency is steeper as a/L grows.

Stiffness and Stability: The increase in modal frequency with larger section sizes reflects improved stiffness and structural stability under dynamic loads. Thus, using larger cross-sections with appropriately designed bracing systems can significantly enhance the vibrational performance of a structure.

Twist Reduces with Increasing a/L: The second graph shows that as the unbraced length ratio (a/L) increases, the amount of twist in all section types decreases. For instance, for HW150x150, the twist starts at 0.08 radians at a/L = 0.05 and reduces to about 0.02 radians by a/L = 0.35. This indicates that increasing the spacing between braces leads to less torsional deformation, possibly due to a more even distribution of forces along the length of the structure.

Larger Sections Exhibit less Twist: Larger sections, such as HW350x350, show much lower values of twist compared to smaller sections like HW150x150. For instance, HW350x350 starts at about 0.04 radians and decreases to 0.01 radians at a/L = 0.35. This trend indicates that larger cross-sectional areas resist twisting more effectively due to their higher torsional stiffness.

Bracing Configuration: The bracing pattern (represented by a/L) also plays a crucial role in improving both modal frequency and twist behaviour. Increasing the unbraced length (a/L) generally leads to better performance in terms of reducing twist and increasing modal frequency. However, this is particularly effective in larger sections, emphasizing the need for strategic bracing placement in combination with appropriately sized structural elements. The use of a knee bracing reduces twisting by nearly four times. After implementing the improved bracing scheme, the structures own weight can be reduced by another 5-6%. For existing structure the total saving in material is approximately 186 kN which costs around 22 to 25 lacs Indian rupees as per current rate.

5.0 Abbreviations

MSW: Modelled Structural Weight

NMSW: Non Modelled Structural Weight

NOC: Normal Operating Condition

EOC: Extreme Operating Condition

FPSO: Floating Platform Storage Offloading

MOW: Mechanical Operating Weight

POW: Piping Operating Weight

NOAX: Normal Operating Acceleration in X direction

NOAY: Normal Operating Acceleration in Y direction

NOAZ: Normal Operating Acceleration in Z direction

EIW: Electrical and Instrumentation Weight

PDW: Piping Dry Weight

POW: Piping Operating Weight

MDW: Mechanical Dry Weight

MOW: Mechanical Operating Weight

DL: Dead Load

LL: Live Load

WL: Wind Load

6.0 Declarations

The authors declare that they have no known competing financial interests or personal relationships that could have appeared to influence the work reported in this paper.

7.0 Availability of Data and Material

The datasets used and/or analysed in the current work are accessible from the corresponding author upon reasonable request.

8.0 Authors Contributions

AY collected the data and contributed significantly to the manuscripts drafting. MK handled the improvements and supervised them. DI helped in paper formatting and content writing. All authors reviewed and approved the final manuscript.

9.0 References

1. API RP 2A-WSD. Recommended practice for planning, designing and constructing fixed offshore platforms-Working stress design. 21st ed; 2000.
2. Babaei M, Moharrami H. Geometry and sizing optimization of steel gable frames with tapered members. Struct. 2022; 42:575-585. https://doi.org/10.1016/j.istruc.2022.05.094
3. Chen Z, Mo L, Li S, Liang Y, Xu D. Seismic behavior of steel reinforced concrete L-shaped columns under compression-bending-shear-torsion combined action. J Build Eng. 2021; 42:102498. https://doi.org/10.1016/j.jobe.2021.102498
4. Das G, Das PJ, Deb SK. Seismic retrofit of torsionally coupled RC soft-storey building using short yielding core BRBs. J Build Eng. 2023; 65:105742. https://doi.org/10.1016/j.jobe.2022.105742
5. Deng R, Zhou XH, Wen H, Li RF, Ji WD. Torsional behaviour of tapered concrete-filled double-skin steel tubular columns with large hollow ratios. Thin-Walled Struct. 2023; 183:110343. https://doi.org/10.1016/j.tws.2022.110343
6. Devi SV, Singh TG, Singh KD. Cold-formed steel square hollow members with circular perforations subjected to torsion. J Constr Steel Res. 2019; 162:105730. https://doi.org/10.1016/j.jcsr.2019.105730
7. Gaoa X, Lia Y, Lib J, Xu J. Effect of steel braces buckling on inelastic torsion and design prevention of steel braced concrete frame structure. 2020; 28:1687-1700. https://doi.org/10.1016/j.istruc.2020.08.048
8. Ghandi E, Niari SE. Flexural-torsional buckling of cold-formed steel columns with arbitrary cross-section under eccentric axial load. Struct. 2020; 28:2122-2134. https://doi.org/10.1016/j.istruc.2020.09.081
9. Hassan RF, Al-Salim NH, Mohammed NS, Hussein HH. Experimental study and theoretical prediction on torsional strength with different steel fiber reinforced concretes and cross-section areas. Eng Struct. 2022; 251(Part A):113559. https://doi.org/10.1016/j.engstruct.2021.113559
10. Hu Z, Wang E, JiaF, Dong M. Experimental study on effect of additional torsional load on bending fatigue behavior and failure mechanism of steel wire rope. Int J Fatigue. 2023; 167(Part B):107399. https://doi.org/10.1016/j.ijfatigue.2022.107399
11. Huang Z, Zhang Y, Huang X, Li Z, et al. Stability of equal-leg angle section braces with torsional restraints. J Constr Steel Res. 2023; 201:107717. https://doi.org/10.1016/j.jcsr.2022.107717
12. Kosin M, Major I, Major M, Kalinowski J. Model tests of bending and torsional deformations of thin-walled profiles stiffened with elements made in 3D printing technology. CSCM. 2020; 13:e00401. https://doi.org/10.1016/j.cscm.2020.e00401
13. Melchera J, Karmazinova M. On problems of torsion analysis of steel members with open cross section. Procedia Eng. 2012; 40:262-267. https://doi.org/10.1016/j.proeng.2012.07.091
14. Nie X, Wang W, Wang YH, Yu J, Hou C. Ultimate torsional capacity of steel tube confined reinforced concrete columns. J Constr Steel Res. 2019; 160:207-222. https://doi.org/10.1016/j.jcsr.2019.05.034
15. Ozer E, Inel M, Cayci BT. Seismic behavior of LRB and FPS type isolators considering torsional effects. Struct. 2022; 37:267-283 https://doi.org/10.1016/j.istruc.2022.01.011
16. Pashaie MR, Mohammadi M. An extended multiple-strut model to estimate infill effects on multi-storey steel frames with different connection rigidities. Struct. 2021; 30:710-734. https://doi.org/10.1016/j.istruc.2020.12.035
17. Pham PV. An innovated theory and closed form solutions for the elastic lateral torsional buckling analysis of steel beams/columns strengthened with symmetrically

balanced GFRP laminates. Eng Struct. 2022; 256:114046. https://doi.org/10.1016/j.engstruct.2022.114046
18. Wang WD, Jia ZL, Shi YL, Tan EL. Performance of steel-reinforced circular concrete-filled steel tubular members under combined compression and torsion. J Constr Steel Res. 2020; 173:106271. https://doi.org/10.1016/j.jcsr.2020.106271.
19. Wang YH, Bai JL, Deng XW, et al. Experimental study on tapered concrete-filled double skin steel tubular columns under torsion. Thin-Walled Struct. 2022; 177:109444. https://doi.org/10.1016/j.tws.2022.109444
20. Xu A, Li S, Fu J, Misra A, Zhao R. A hybrid method for optimization of frame structures with good constructability. Eng Struct. 2022; 276:115338. https://doi.org/10.1016/j.engstruct.2022.115338
21. Yadhav A, Gosavi S, Kulkarni M. Nonlinear behaviour of a reinforced concrete building subjected to blast load and optimisation using a meta-heuristic algorithm. AJCE. 2024; 25:397-412. https://doi.org/10.1007/s42107-023-00783-2
22. Yadhav A, Kulkarni M. Optimal design of FPSO topside module for in-place, lift and weighing conditions utilizing meta-heuristic optimization algorithms. Asian J Civ Eng. 2023; 24:3055-3070. https://doi.org/10.1007/s42107-023-00694-2